Interference Reduction in LiFi Using an Optical Receiver with Dynamic FoV

Mohammad Dehghani Soltani, Iman Tavakkolnia, Harald Haas
LiFi Research and Development Centre, Electrical Engineering Division, Department of Engineering,
The University of Cambridge, Cambridge, UK
Email: {md2104, it360, huh21}@cam.ac.uk

***Abstract*—In optical wireless communication (OWC) networks, managing interference and enhancing data rates are critical challenges, particularly in environments with multiple users. This paper investigates the impact of the receiver's field of view (FoV) on interference reduction and signal-to-interference-plus-noise ratio (SINR) improvement in light-fidelity (LiFi), which is a networked OWC system. A narrower FoV can effectively limit the reception of unwanted signals, thereby mitigating inter-user interference and enhancing SINR. This work explores how FoV optimization contributes to interference suppression while maximizing SINR. Additionally, the integration of liquid crystal lenses (LCL) to the receiver permits a dynamic FoV for achieving interference-resistant communication. LCLs adjust the focus by applying an electric field to them, and have faster response time in comparison to the coherence time of LiFi. By incorporating realistic scenarios, including both line-of-sight (LoS) and non-LoS (NLoS) propagation, as well as random device orientations, and formulating an optimization problem to determine the optimal FoV, this study provides valuable insights for designing interference-resistant and high-performance LiFi systems. The results emphasize that employing a dynamic FoV enhances the average SINR by approximately 4 dB across the entire room, even under random device orientations. Moreover, configuring the receiver with a dynamic FoV range between 40° to 55° consistently yields high SINR throughout the room.**

***Index Terms*—Optical wireless communications, Interference mitigation, Field-of-view (FoV), Mobility, Connectivity.**

I. Introduction

The surging demand for wireless data has driven both academia and industry to explore alternative technologies capable of delivering efficient, reliable, and high-speed wireless services. Light-fidelity (LiFi) is a networked optical wireless communication represents a key component of future indoor wireless systems. LiFi leverages visible light as the propagation medium to transmit information, utilizing off-the-shelf light-emitting diodes (LEDs) as optical sources and photodiodes (PDs) as detectors [1]. LiFi offers lowers energy consumption by enabling simultaneous illumination and data communication. Moreover, LiFi reduces electromagnetic interference and spectrum congestion, contributing to improved network sustainability. Given the increasing demand for high-speed, low-power communication, LiFi plays a crucial role in minimizing the carbon footprint of future networks [2].

To unlock the full potential of LiFi systems, the optical link between the access point (AP) and user equipment (UE) must be carefully optimized. In a multi-user scenario, the receiver's field of view (FoV) plays a pivotal role in mitigating interference and optimizing network performance [3]. A narrower FoV reduces the reception of unwanted signals from extraneous sources, thereby enhancing the SINR. Conversely, a broader FoV increases the likelihood of interference, especially in multi-user settings, but may improve coverage [4]. Thus, optimizing the FoV of optical receivers is essential for balancing interference reduction with the ability to maintain connectivity and maximize data throughput [5].

Techniques such as angle diversity receiver [6], fractional frequency reuse (FFR) [7], spatial filtering [8] and beamforming [9] are used in optical wireless communication (OWC) to mitigate the co-channel interference. In [6], the interference mitigation performance of pyramid receivers and truncated pyramid receivers with an optimized lower bound on the FoV for each PD are examined. In [7], an FFR technique is introduced as a low-complexity solution that reduces interference of users at the cell edge. In [8], a spatial light modulator is introduced in the form of a liquid crystal panel to filter out ambient and modulated light interference. In [9] a dynamic beam pattern adjustment is proposed using linear array antennas to mitigate femtocell interference, achieving approximately a 5% improvement in spectral efficiency compared to fixed power control schemes. Recent advancements in adaptive FoV control, and hardware innovations such as variable focus lenses have opened new avenues for dynamic interference management in OWC systems [3]. By employing a dynamic FoV significant improvements in reducing inter-cell interference, boosting data rates, and maintaining robust connectivity is demonstrated [10], [11]. Dynamic FoV can be implemented by employing adaptive liquid crystal lenses (LCL) that adjust the receiver's field of view in real time based on the prevailing environmental conditions [12]. LCLs adjust focus by applying an electric field that modulates the refractive index of the lens material, thereby altering the lens focus in real time. Their response time is significantly faster than the coherence time of LiFi, enabling rapid adaptation to dynamic channel conditions [13]. An electronically controlled compact liquid lens for designing a dynamic FoV optical receiver was first implemented and tested in [14]. Their experimental results demonstrate that their proposed dynamic FoV receiver significantly enhances SINR compared to a fixed FoV receiver. Additionally, it offers a more compact, energy-efficient, and faster alternative to traditional mechanical solutions.

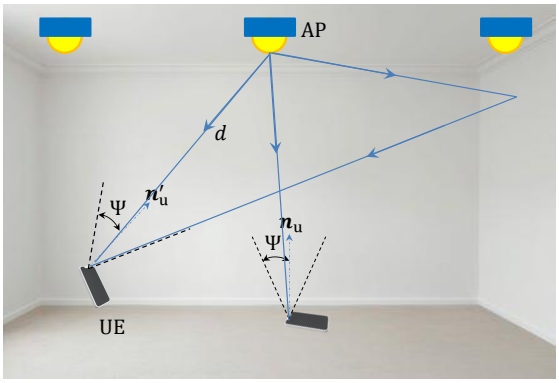

Fig. 1. Downlink geometry of light propagation in LiFi networks.

This paper explores the impact of receiver FoV optimization on interference reduction and rate improvement in optical wireless networks. By drawing on existing research and leveraging real-world scenarios, we aim to provide insights into how FoV adjustments can transform the design and deployment of next-generation OWC systems. The findings contribute to the ongoing development of scalable, efficient, and interference-resistant communication networks, meeting the growing demands for reliable high-speed connectivity in diverse applications. The contributions of this study are fourfold: 1. A comprehensive analysis of the impact of the FoV on interference and SINR is conducted, providing a deeper understanding of system performance. 2. Realistic scenarios, such as NLoS propagation and random device orientations, are incorporated into the simulations to ensure practical relevance and accuracy. 3. An optimization problem is formulated to determine the optimal FoV that minimizes the interference power, and the statistics of this optimal FoV are analyzed across various room locations and device orientations. 4. Insightful results are presented, accompanied by detailed discussions on the influence of various parameters on interference, offering valuable guidance for system design and optimization.

II. System Model

A. LiFi Channel Model

We consider an indoor optical attocell network consisting of multiple APs acting as transmitters and multiple optical receivers. In this setup, an LED serves as the optical source, while a PD functions as the detector. Given the incoherent nature of LEDs, the most practical approach for modulation and down-conversion in LiFi is intensity modulation with direct detection (IM/DD), where the signal is encoded onto the power of the optical carrier. This technique ensures simplicity and effectiveness for LiFi systems. Figure 1 shows the downlink geometry of light propagation in LiFi networks.

The OWC channel is characterized by the presence of both line-of-sight (LoS) and non-line-of-sight (NLoS) components, where LoS refers to a direct and unobstructed link between an AP and a UE, while the NLoS link relies on light reflections from surfaces such as walls and furniture within the environment. Consequently, the optical channel in an indoor OWC system can be described as follows:

$$H = H_{\text{LoS}} + H_{\text{NLoS}}, \tag{1}$$

where H_{LoS} and H_{NLoS} are the direct-current (DC) gain of the LoS and NLoS links, respectively. The DC gain of the LoS path between the AP and the UE is given by:

$$H_{\text{LoS}} = v\frac{(m+1)A}{2\pi d^2}\cos^m\phi\cos\psi, \tag{2}$$

where A, ϕ, and ψ are the detector area, the transmitter radiance angle, and the receiver incidence angle, respectively. The Lambertian order, m, is defined as $m = -\frac{1}{\log_2(\cos\Phi_{1/2})}$, where $\Phi_{1/2}$ is the half-intensity angle. The visibility factor, v is 1 for $0 \le \psi \le \Psi$ and 0, otherwise where Ψ is the FoV. The radiance angle, ϕ and the incidence angle, ψ can be calculated by $\cos\phi = \frac{d.\mathbf{n}_t}{||d||}$ and $\cos\psi = \frac{-d.\mathbf{n}_u}{||d||}$. $\mathbf{n}_t = [0,0,-1]^T$ and $\mathbf{n}_u = [0,0,1]^T$ are the normal vectors at the AP and UE, respectively while d is the distance vector from the UE to the AP. The symbols $.$, $||\,.\,||$ and $(.)^T$ are the inner product, the Euclidean norm operators and the transpose operator, respectively.

For NLoS links, obtaining accurate values for the diffuse channel components necessitates considering a high reflection order. To address this challenge, we employ the method proposed in [15], which accounts for an infinite order of reflections by calculating the channel gain in the frequency domain rather than the time domain. In this approach, the environment is partitioned into small surface elements, each serving as a reflector. Consequently, the NLoS channel gain, which incorporates an infinite number of reflections, can be expressed as:

$$H_{\text{NLoS}} = \mathbf{r}^T\mathbf{G}_\rho(\mathbf{I} - \mathbf{H}_e\mathbf{G}_\rho)^{-1}\mathbf{t}, \tag{3}$$

where the transmitter transfer function vector, denoted as $\mathbf{t} = [H_{1,\text{Tx}}, H_{2,\text{Tx}}, \ldots, H_{N,\text{Tx}}]^T$, describes the transfer functions of the transmitter. The frequency-dependent matrix, $\mathbf{H}_e$, represents the LoS transfer function between the kth and ith reflectors, where the reflectors act as the transmitter and receiver surface elements, respectively. The receiver transfer function vector, $\mathbf{r}$, is given by $\mathbf{r}^T = [H_{\text{Rx},1}, H_{\text{Rx},2}, \ldots, H_{\text{Rx},N}]$. The reflectivity matrix $\mathbf{G}\rho = \text{diag}(\rho_1, \rho_2, \ldots, \rho_N)$ includes the reflection coefficients ρ_i of the ith reflector, while $\mathbf{I}$ is the unity matrix of size $N \times N$.

B. Random Orientation Model

In LiFi systems, the channel gain is highly influenced by the random orientation of the UE. Therefore, it is crucial to account for this factor to develop an accurate and realistic channel model. In [16], the authors proposed a novel model for the random orientation of mobile devices, which we adopt for modeling the indoor channel of our system. According to this model, the incidence angle ψ can be expressed as: $\cos\psi = a\sin\theta + b\cos\theta$ with $a = -\left(\frac{x_a - x_u}{d}\right)\cos\Omega - \left(\frac{y_a - y_u}{d}\right)\sin\Omega$ and $b = \left(\frac{z_a - z_u}{d}\right)$. Here, (x_a, y_a, z_a) and (x_u, y_u, z_u) represent the location vectors of the AP and the UE, respectively. The parameter θ denotes the elevation angle between the positive direction of the Z-axis and the UE's normal vector, while Ω

represents the facing direction of the UE. This formulation allows us to incorporate $\cos\psi$ directly into the channel gain analysis, enabling a more accurate representation of the impact of random device orientation on system performance.

III. SINR Calculation

In communication systems, SINR is the ratio of the desired signal power to the total noise and interference power. It is a critical metric for assessing link quality and determining the achievable data rate. The SINR of the UE served by AP_t is given by:

$$\mathrm{SINR} = \frac{P_{\mathrm{elec}}}{\sigma^2 + P_{\mathrm{int}}}, \tag{4}$$

where P_{elec} represents the received electrical power at the UE; $\sigma^2 = N_0 B/K$, denotes the noise power, with N_0 being the noise power spectral density; and P_{int} accounts for interference from other APs at the UE. Additionally, B denotes the downlink bandwidth. It is assumed that all APs emit the same average optical power. The received electrical power at the UE is given by:

$$P_{\mathrm{elec}} = R^2 P_{\mathrm{t}}^2 H_t^2 \tag{5}$$

where P_{t} denotes the transmitted optical power, R represents the PD responsivity, and H_t is the channel gain between the serving AP and the UE. The channel gain accounts for both LoS and NLoS components. Consequently, the received SINR is given by:

$$\mathrm{SINR} = \frac{R^2 P_{\mathrm{t}}^2 H_t^2}{\sigma^2 + \sum\limits_{i \in \Xi_{\mathrm{AP},t}} R^2 P_{\mathrm{t}}^2 H_i^2}. \tag{6}$$

where $\Xi_{\mathrm{AP},t}$ represents the set of all APs in the room except for the serving AP, i.e., AP_t.

IV. Dynamic FoV Solution

A narrow FoV effectively reduces interference but may inadvertently exclude desired signals, particularly in NLoS scenarios. On the other hand, a wide FoV increases interference power due to the inclusion of additional APs within the receiver's FoV. By employing a receiver with a dynamic FoV, as opposed to a fixed FoV, the system can dynamically adjust the FoV to exclude interfering APs while prioritizing relevant signals. This adaptability significantly alleviates interference power and enhances the SINR, leading to improved overall system performance. The challenge here would be how to optimize the FoV. In the following, we provide a mathematical framework for FoV optimization. The interference power P_{int} at a UE can be expressed as:

$$P_{\mathrm{int}} = \sum_{i \in \Xi_{\mathrm{AP},t}} R^2 P_{\mathrm{t}}^2 H_{i,j,k}^2 \tag{7}$$

When the FoV is dynamically adjusted, the number of APs contributing to interference changes, directly affecting P_{int}. To minimize interference while maintaining a target SINR,$\mathrm{SINR}_{\mathrm{req}}$, the FoV, Ψ can be optimized. The optimization problem can be formulated as:

$$\min_{\Psi} \quad P_{\mathrm{int}} \tag{8a}$$

$$\text{s.t.} \quad \Psi \geq \Psi_{\min}, \tag{8b}$$

$$\mathrm{SINR} \geq \mathrm{SINR}_{\mathrm{req}}, \tag{8c}$$

where $\Psi_{\min}$ is the minimum FoV.

By dynamically adjusting the FoV of the receiver, the impact of interference from unwanted sources can be minimized without compromising the required data rate. The optimal FoV at each location depends not only on the device's spatial coordinates but also on its orientation.

Implementing a dynamic FoV in a LiFi receiver requires adjustable optics or electronically controlled elements to adapt the receiver's aperture in response to signal quality variations. One practical approach is using liquid crystal-based tunable lenses, which can modify the FoV by adjusting the refractive index when an external voltage is applied [14]. Another method involves microelectromechanical systems (MEMS) micromirrors, which can dynamically steer the optical path to optimize signal reception [17], [18]. Additionally, an array of photodetectors with selective activation can enable adaptive FoV control by choosing the most favorable sensing elements based on signal strength and interference levels. These techniques can achieve FoV adjustments within milliseconds to a few tens of milliseconds, depending on the actuation mechanism [19]. Compared to UE orientation and movement, which typically occur on a timescale of hundreds of milliseconds to seconds [20], dynamic FoV adaptation can be significantly faster, allowing the receiver to swiftly optimize performance in response to channel variations without being constrained by the UE's motion dynamics.

TABLE I
LiFi Simulation Parameters

Parameter	Symbol	Value
Room dimension	-	$6 \times 6 \times 3$
Number of APs	-	4
LED half-intensity angle	$\Phi_{1/2}$	45°, 60°
Receiver FoV	Ψ	variable
Receiver physical area	A	0.5×0.5 cm^2
PD responsivity	R	1 A/W
Wall reflection coefficient	ρ	0.8
Ceiling reflection coefficient	ρ	0.6
Floor reflection coefficient	ρ	0.3
Transmitted optical power	P_{t}	1 W
Noise power spectral density	N_0	10^{-21} A^2/Hz
Downlink transmission bandwidth	B	10 MHz

V. Simulation Results

The simulations are performed for a network area measuring $6 \times 6 \times 3\,\mathrm{m}^3$. The area is evenly divided into four quadrants, with an AP positioned at the center of each quadrant. The receiver height is set to 0.85 m for all simulations. The bandwidth of the LED, depending on the applications, can vary from several MHz, for standard LEDs, to a few GHz, for high-speed LEDs. In this study, we have selected a commercial LED with a

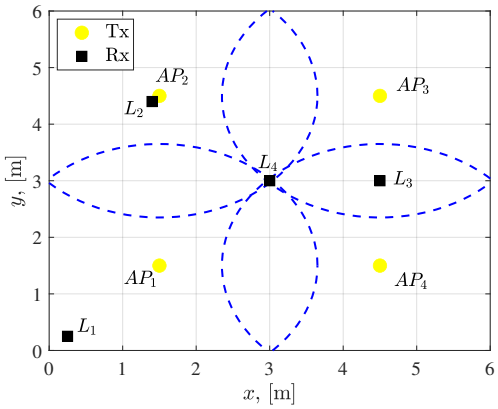

Fig. 2. AP and UE arrangements in the room.

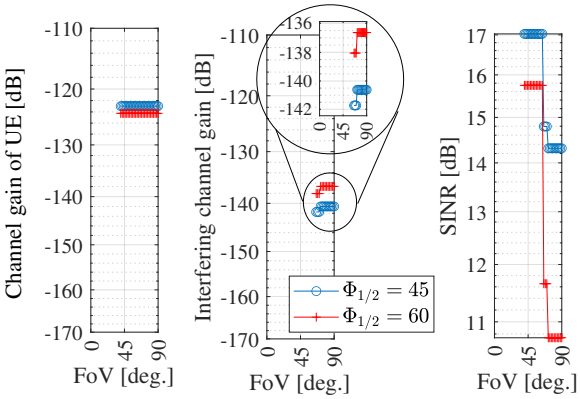

Fig. 3. Comparison of channel gains and SINR when only LoS is considered. The UE is located at L_1.

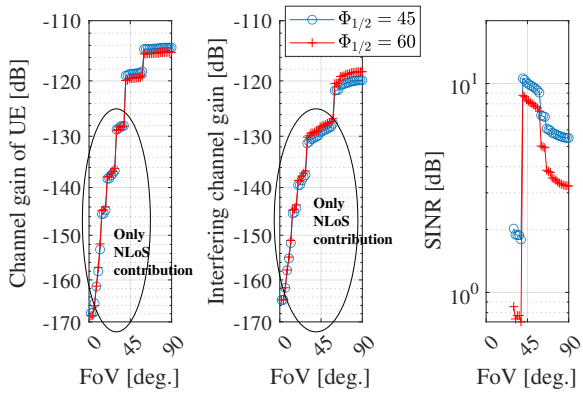

Fig. 4. Comparison of channel gains and SINR when both LoS and NLoS are considered. The UE is placed at L_1.

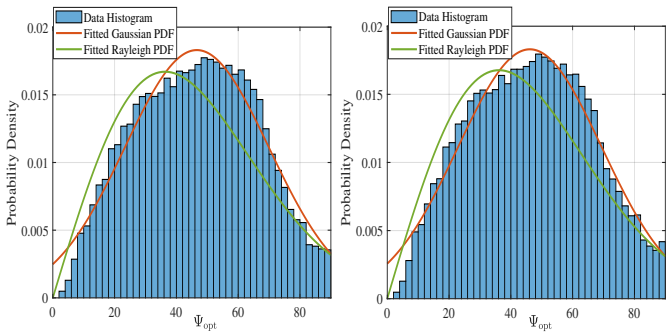

(a) $\Phi_{1/2} = 45°$ (b) $\Phi_{1/2} = 60°$

Fig. 5. Impact of LED half-intensity angle on the statistics of optimum FoV.

bandwidth of 10 MHz. The rest of the parameters are presented in Table I. We first compared the results for a LoS channel and then extended the analysis to include NLoS components. The comparison highlights the importance of incorporating realistic channel conditions, including both LoS and NLoS to more accurately assess network performance and optimize receiver design.

Figure 3 compares the LoS-only channel gain for the UE positioned at the corner of the room, L_1, and connected to AP_1. The results are presented for two LED half-intensity angles of 45° and 60°. From Fig. 3a, it is evident that in both cases, the LoS channel gain becomes zero when the FoV is less than $\Psi_{\min} \approx 40°$. As shown in Fig. 3b, the interfering channel gain initially increases and then remains constant as the FoV expands. This behavior occurs because the UE first detects AP_2 and AP_4 when the FoV reaches 66°. As FoV increases further to 72°, the UE additionally detects AP_3, resulting in an abrupt rise in the interfering channel gain. Fig. 3c illustrates the SINR values for LED half-intensity angles of 45° and 60°. The initial decline in SINR occurs as the device's FoV increases, enabling it to first detect AP_2 and AP_4. The subsequent decline in SINR is attributed to the device eventually detecting AP_3 as the FoV continues to expand.

Figure 4 illustrates the channel gain incorporating both LoS and NLoS components for the UE positioned at L_1 and connected to AP_1. For FoVs below $\Psi\min \approx 40°$, the channel gain remains non-zero due to the contribution of NLoS components. As the FoV increases, the receiver captures more power from reflections off walls and the ceiling, leading to a higher channel gain, as shown in Fig. 4a. Comparing this to the channel gain of the UE in Fig. 3, a difference of 8 dB and 9 dB is observed for $\Phi_{1/2} = 45°$ and $\Phi_{1/2} = 60°$, respectively. Fig. 4b presents the interfering channel gain. Up to a FoV of 66°, only the NLoS components contribute to the interfering channel gain. As the FoV increases, interference from other APs also rises, reaching approximately -120 dB and -118 dB at a FoV of 90° for $\Phi_{1/2} = 45°$ and $\Phi_{1/2} = 60°$, respectively. The SINR results, shown in Fig. 4c, indicate the presence of an optimal FoV angle that balances the received power and interference from neighboring APs. At first, and up to a FoV of 40°, only NLoS channels contribute to the SINR. As observed, the SINR initially decreases because the interfering channel gain becomes more significant than the main channel gain, causing a continued decline in SINR. However, when the FoV reaches 40°, the UE detects the LoS channel gain from AP_1, resulting in a sudden increase in SINR. Beyond this point, as the FoV further increases, the SINR gradually decreases because the collected power from interfering channels becomes more dominant than the received power from AP_1.

Fig. 5 represents the PDF of optimum FoV over different locations of the room. For these results, the device random

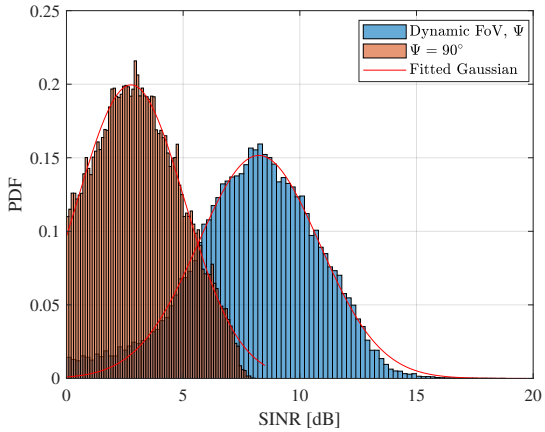

Fig. 6. PDF of SINR with random orientation over the whole room for a receiver with dynamic FoV, Ψ and a receiver with fixed FoV of $\Psi = 90°$.

orientation is considered where θ and Ω are modeled as a Laplace and a uniform distribution, respectively, with the parameters given in [21]. Both LoS and NLoS channel gains are considered in these results. The results are shown for two LED half angles, $\Phi_{1/2}$, of 45° and 60°. The optimum FoV, Ψ_{opt}, is calculated based on the optimization problem given in (8) at each location and for each orientation of the device. The required data rate, R_{req}, is set to 5 MHz. If more than two FoVs meet the rate requirement, the FoV that maximizes the rate is selected as Ψ_{opt}. Two distributions, i.e., truncated Rayleigh and truncated Gaussian, are fitted to the PDF of Ψ_{opt}, as can be seen, the distribution of Ψ_{opt} is more like a truncated Gaussian one, with a mean of 45.48° and 45.30° for $\Phi_{1/2} = 45°$ and $\Phi_{1/2} = 60°$, respectively. The results highlight that approximately 68% of the optimal FoV values fall within the range of 26° to 65°. Utilizing a truncated Gaussian distribution enables designers to optimize the dynamicity and adaptability of receiver FoV effectively, ensuring they meet the desired SINR and rate requirements.

Fig. 6 shows the SINR PDF across the entire room, considering device random orientation, for two cases: when the FoV is set to the optimal value, $\Psi = \Psi_{\text{opt}}$, determined from the optimization problem, and when the FoV is fixed at $\Psi = 90°$. For both cases, we have set the LED half-intensity angle to 45°. The FoV is assumed to be dynamic, ranging from 26° to 65°, i.e., $\Psi \in [26°, 65°]$, based on the results shown in Fig. 5. The first notable observation from these results is that the SINR for $\Psi = 90°$ is most likely below 7 dB, whereas for $\Psi = \Psi_{\text{opt}}$, the SINR can reach as high as 15 dB. These findings suggest that deploying four APs in a room of size 6×6 results in a mean SINR of 8 dB. To further enhance the SINR, it is recommended to employ techniques such as frequency reuse, deploying additional APs with narrower LED half-intensity angles, or utilizing IRS in scenarios where the UE faces walls and relies primarily on the NLoS channel [22]. Additionally, the SINR distribution follows a truncated Gaussian pattern, which is well-fitted to the PDF of the SINR.

Fig. 7 illustrates the SINR distribution across the entire room for a UE with a dynamic FoV, oriented vertically upward. The

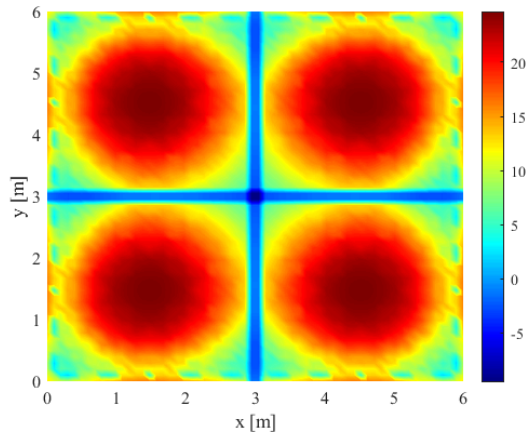

Fig. 7. SINR [dB] distribution over the room, for a receiver with dynamic FoV. The UE is vertically upward.

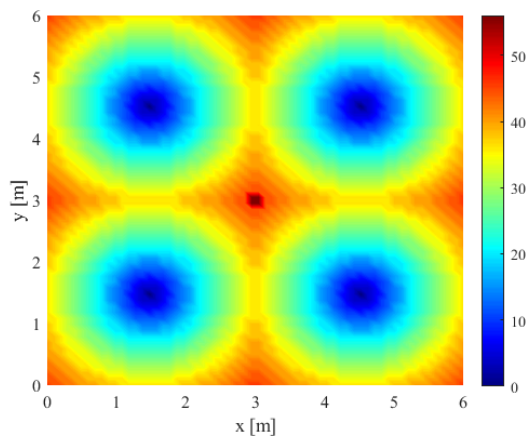

Fig. 8. optimum FoV [Deg.] distribution over the room obtained from Eq. 8, when UE is vertically upward.

LED half-intensity angle is $\Phi_{1/2} = 60°$. The results confirm that the maximum SINR occurs directly beneath each AP and decreases as the UE moves toward the cell boundaries. The minimum SINR is observed at the center of the room, as expected, due to high interference power. Fig. 8 depicts the optimal FoV value that maximizes the SINR, which were shown in Fig. 7.

Fig. 9 illustrates the SINR distribution across the entire room for a UE with a dynamic FoV, considering the effect of random device orientation, with an elevation angle of $\theta = 41°$ [16]. The LED half-intensity angle is $\Phi_{1/2} = 60°$. Unlike previous results, the presence of random orientation reveals that the maximum SINR does not occur directly beneath each AP. Instead, the maximum SINR forms a doughnut-shaped region rather than being centered below the AP. The minimum SINR is observed at the center of the room, similar to previous findings, due to the high interference power in that region. Fig. 10 shows the mean optimal FoV value, i.e., $\mathbb{E}_\theta[\mathbb{E}_\Omega[\Psi_{\text{opt}}]]$, for each location of the room that maximizes the SINR, as presented in Fig. 9.

VI. Conclusion

In this paper, we investigated the critical role of receiver FoV optimization in mitigating interference and enhancing SINR

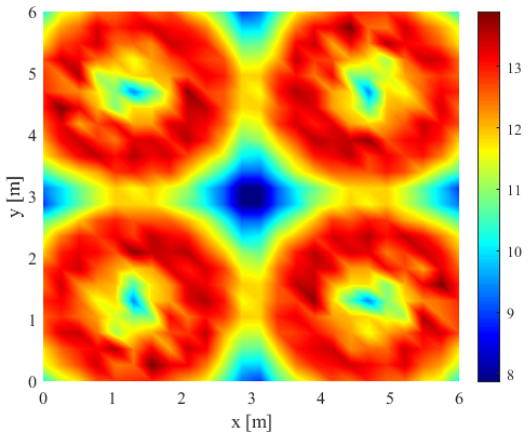

Fig. 9. SINR [dB] distribution over the room, for a receiver with dynamic FoV. The random orientation of UE is implemented.

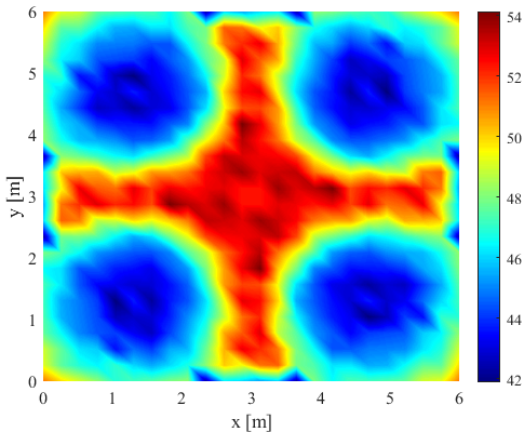

Fig. 10. Mean value of optimum FoV [Deg.], $\mathbb{E}_\theta[\mathbb{E}_\Omega[\Psi_{\text{opt}}]]$, distribution over the room obtained from Eq. 8, with consideration of random orientation.

in LiFi systems. Our analysis, which incorporated both LoS and NLoS propagation as well as random device orientations, revealed that a optimized FoV can effectively suppress unwanted signals, leading to significant improvements in network performance. By formulating an optimization problem to determine the optimal FoV and analyzing its statistics across diverse scenarios, we have provided in-depth insights that can offer valuable guidance for the development of interference-resilient communication networks. The results demonstrate that implementing a dynamic FoV improves the average SINR across the entire room by approximately 4 dB, even with random device orientations. Additionally, configuring the receiver with a dynamic FoV range between 40° and 55° is sufficient to consistently achieve high SINR throughout the room.

Acknowledgment

This work was supported by the Future Telecoms Research Hubs, Platform for Driving Ultimate Connectivity (TITAN) and the Hub for All Spectrum Connectivity, sponsored by the Department of Science Innovation and Technology (DSIT) and the Engineering and Physical Sciences Research Council (EPSRC) under Grant EP/X04047X/1, EP/Y037243/1, EP/X040569/1, and EP/Y037197/1.

References

[1] T. Komine and M. Nakagawa, "Fundamental analysis for visible-light communication system using led lights," *IEEE Trans. Consum. Electron.*, vol. 50, pp. 100–107, Feb 2004.

[2] A. B. Ozyurt, R. Bian, H. Haas, and W. O. Popoola, "Energy and Spectral Efficiency of Multi-Tier LiFi Networks," in *2023 IEEE Wirel. Commun. Netw. Conf. (WCNC)*, pp. 1–6, 2023.

[3] M. W. Eltokhey, M. A. Khalighi, and Z. Ghassemlooy, "Optimization of Receivers' Field of Views in Multi-User VLC Networks: A Bio-Inspired Approach," *IEEE Wirel. Commun.*, vol. 29, no. 2, pp. 132–139, 2022.

[4] Shashikant, P. Garg, and P. K. Sharma, "Interference Mitigation Technique with Coverage Improvement in Indoor VLC System," *Trans. Emerg. Telecommun. Technol.*, vol. 30, no. 2, p. e3511, 2019.

[5] I. Abdalla, M. B. Rahaim, and T. D. C. Little, "Interference Mitigation Through User Association and Receiver Field of View Optimization in a Multi-User Indoor Hybrid RF/VLC Illuminance-Constrained Network," *IEEE Access*, vol. 8, pp. 228779–228797, 2020.

[6] Z. Zeng *et al.*, "Interference Mitigation Using Optimised Angle Diversity Receiver in LiFi Cellular Network," *Opt. Commun.*, vol. 574, p. 131125, 2025.

[7] C. Chen, N. Serafimovski, and H. Haas, "Fractional Frequency Reuse in Optical Wireless Cellular Networks," in *2013 IEEE 24th Annu. Int. Symp. on Personal, Indoor, and Mobile Radio Commun. (PIMRC*, pp. 3594–3598, 2013.

[8] C. Tebruegge, Q. Zhang, and F. Dressler, "Optical Interference Reduction with Spatial Filtering Receiver for Vehicular Visible Light Communication," in *2019 IEEE Intell. Transp. Syst. Conf. (ITSC)*, pp. 3055–3061, 2019.

[9] K. S. Mohamed, M. Y. Alias, and M. Roslee, "Interference Management Using Beamforming Techniques for Line-of-Sight Femtocell Networks," *IEICE Trans. Commun.*, vol. 103, no. 8, pp. 881–887, 2020.

[10] I. Abdalla, M. Rahaim, and T. Little, "On the importance of dynamic fov receivers for dense indoor optical wireless networks," in *IEEE Int. Conf. Commun. (ICC), 2020*, pp. 1–6, 2020.

[11] A. Krohn, A. Harlakin, S. Arms, S. Pachnicke, and P. A. Hoeher, "Impact of Liquid Crystal Based Interference Mitigation and Precoding on the Multiuser Performance of VLC Massive MIMO Arrays," *IEEE Photonics J.*, vol. 14, no. 5, pp. 1–12, 2022.

[12] Z. wei Ye, Y. yu Zhang, C. Wang, P. hui Fan, and Y. jun Zhu, "RIS-Aided Dynamically Adaptive Wide Field-of-View Receiver for Visible Light Communication in Industrial Internet of Things," *Opt. Express*, vol. 31, pp. 34748–34763, Oct 2023.

[13] V. N. Y. N. J. V. O. Kurochkin, O. Buluy and M. Manevich, "Ultra-Fast Liquid Crystal Lens with Variable Focal Length," *Molecular Crystals and Liquid Crystals*, vol. 696, no. 1, pp. 29–42, 2020.

[14] K. Bera and N. Karmakar, "Interference Mitigation in VLC Systems using a Variable Focus Liquid Lens," *Photonics*, vol. 11, no. 6, 2024.

[15] H. Schulze, "Frequency-domain simulation of the indoor wireless optical communication channel," *IEEE Trans. Commun.*, vol. 64, pp. 2551–2562, June 2016.

[16] M. D. Soltani, A. A. Purwita, Z. Zeng, H. Haas, and M. Safari, "Modeling the random orientation of mobile devices: Measurement, analysis and LiFi use case," *IEEE Trans. Commun.*, vol. 67, pp. 2157–2172, March 2019.

[17] L. Li, "MEMS Micromirrors for Imaging Applications," 2013.

[18] S. Xu, Y. Li, Y. Liu, J. Sun, H. Ren, and S.-T. Wu, "Fast-Response Liquid Crystal Microlens," *Micromachines*, vol. 5, no. 2, pp. 300–324, 2014.

[19] S. Mukherjee *et al.*, "Fast Refocusing Lens Based on Ferroelectric Liquid Crystals," *Opt. Express*, vol. 29, pp. 8258–8267, Mar 2021.

[20] T. Tang, L. Shi, and Q. Li, "Mobility Analysis of Visible Light Communications with Orientation-based Random Waypoint Model," in *2024 5th Information Communication Technologies Conference (ICTC)*, pp. 194–198, 2024.

[21] M. D. Soltani, M. A. Arfaoui, I. Tavakkolnia, A. Ghrayeb, M. Safari, C. M. Assi, M. O. Hasna, and H. Haas, "Bidirectional Optical Spatial Modulation for Mobile Users: Toward a Practical Design for LiFi Systems," *IEEE J. Sel. Areas Commun.*, vol. 37, no. 9, pp. 2069–2086, 2019.

[22] M. D. Soltani, X. Wu, M. Safari, and H. Haas, "Bidirectional user throughput maximization based on feedback reduction in LiFi networks," *IEEE Trans. Commun.*, vol. 66, pp. 3172–3186, July 2018.